Mechanical Changes in Materials Caused by Explosive Precompression Shock Waves and the Effects on Fragmentation of Exploding Cylinders

T. Hiroe[1, a], K. Fujiwara[1, b], H. Hata[1, c], K. Watanabe[2, d] and M. Yamamoto[3, e]

[1] Department of Mechanical System Engineering, Kumamoto University, Kumamoto 860-8555
[2]Graduate School of Science and Engineering, Kumamoto University
[3]Technical Division, Faculty of Engineering, Kumamoto University

[a]hiroe@gpo.kumamoto-u.ac.jp, [b]Fujiwara@kumamoto-u.ac.jp, [c]hata@mech.kumamoto-u.ac.jp, [d]064d8539@gsst.stud.kumamoto-u.ac.jp, [e]yfamily@mech.kumamoto-u.ac.jp,

Keywords: Mechanical Properties, Shock Wave Transmission, Momentum Trap, Cylinder Explosion, Fragmentation Energy

Abstract. Explosive driven rapid fracture in a structural body will be preceded by a compression process, and the compression effects on mechanical properties of the materials are clearly important to understand shock-induced failure such as spall or fragmentation phenomena. In this study, incident shock waves in plate specimens of aluminum A2017-T4 and 304 stainless steel are generated by plane detonation waves in the high explosive PETN initiated using wire-row explosion techniques, and the compressed specimens are successfully recovered without severe damages due to the reflected expansion waves with use of momentum trap method. A hydro code, Autodyn-2D is applied to determine test conditions: thicknesses of explosives, attenuators, specimens and momentum traps and to evaluate experimental results, simulating time-histories of stress waves in the layers of the test assembly. Microhardness distributions in cross-sections, tensile strength, fracture ductility and yield stress are measured for the recovered specimens, using miniature tensile and compression test pieces machined from them. They are compared with those of virgin specimens, showing significant increase of hardness, tensile and yield strength and remarkable reduction of elongation and ductility for shocked specimens. The results are taken into consideration for evaluation of experimental fragmentation energy in cylinder explosion tests.

Introduction

The understanding of high-strain-rate deformation and fracture behavior of materials and structural components has been of great importance in safety evaluation and fracture control design for accidental impact of vehicles and crashworthiness shielding, blast of high-energy storage containers and space applications. Such high speed failure phenomena are typically initiated by impacts between solid or gas bodies and strong compressive stress waves are created and transmitted through the bodies prior to the terminal tensile deformation and fracture of structures, but usually such preceded processes have been involved implicitly in the evaluation of posterior fractural phenomena.

Authors had applied wire explosion techniques [1] to produce diverging and planar detonation waves in the powder high explosive pentaerythritoltetranitrate (PETN) for the studies on spall fracture of plates [2] and uniform expansion and fragmentation of cylinders [3, 4] of aluminum alloys and a stainless steel. Experimentally derived values of spall strength [5] and fragmentation energy [6] of materials used for fracture evaluation effectively had been obviously affected by prior strong compressive pulses. In this study, explosively shocked plate specimens of aluminum A2017-T4 and 304 stainless steel are successfully recovered without a large amount of damages due to the reflected expansion waves using momentum traps designed with help of numerical simulations. Measured mechanical properties of the recovered specimens reveal remarkable changes from those of the virgin materials, giving some considerations on the dynamic fracture [2-4, 7] induced by shocks.

Experiments for Recovery of Explosively Precompressed Plates

Test assembly. Explosively loading experiments are performed using the explosion test facilities at the Shock Wave and Condensed Matter Research Center, Kumamoto University. Figure 1 illustrates the developed test assembly for recovery of precompressed plate specimen, which consists of four layers of a PETN slab packed to 0.90-0.95g/cc with attached parallel copper wire-rows (wire dia.: 175μm) for generation of planar detonation [1], an air layer as an attenuator (AT), a circular plate specimen (TP) of A2017-T4 or 18Cr-8Ni stainless steel (JIS SUS304), and a circular momentum trap plate (MT) of the same material as specimen. The PETN are filled up to 15mm and 20mm thick for A2017 and 304SS respectively. The air layer AT of 10mm thickness is inserted in case to transfer lower incident shock pressure only for A2017 specimen. The contact surfaces of specimens and the momentum traps are lapped to superfine finish. A planar detonation front is produced in the PETN layer immediately after simultaneous explosion of wire-rows with use of an impulsive discharge current from a capacitor bank of 40kV, 12.5μF and a triangular-type pressure pulse transfers into TP and MT. It is expected that the TP would be recovered without severe damages with effect of the MT. The thicknesses t_1 and t_2 of provided TP and MT are 5, 10, 15mm: 9 kinds of combinations for A2017 and 10, 15mm: 4 kinds for 304SS and A2017 (AT attached type), and represented as TPt_1MTt_2. All the test conditions are determined using the following numerical results.

Numerical simulations and recovery tests. Numerical simulations were performed for all the experiments using a hydro code: Autodyn 2D based on Finite Difference Method (FDM), where the Steinberg-Guinan model [5] is adopted for the constitutive equation for metals. Figure 2 (a), (b) shows typical numerical time-histories of spatial distributions of normal stress (compressive stress: positive) in the test assembly layers for TP10/MT10 (304SS) and AT10/TP10/MT15 (A2017).

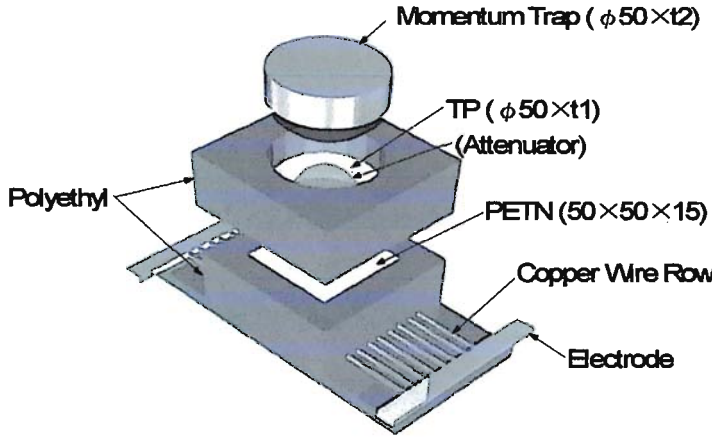

Figure 1. Schematics of test assembly for recovery of explosively precompressed (or shocked) specimens

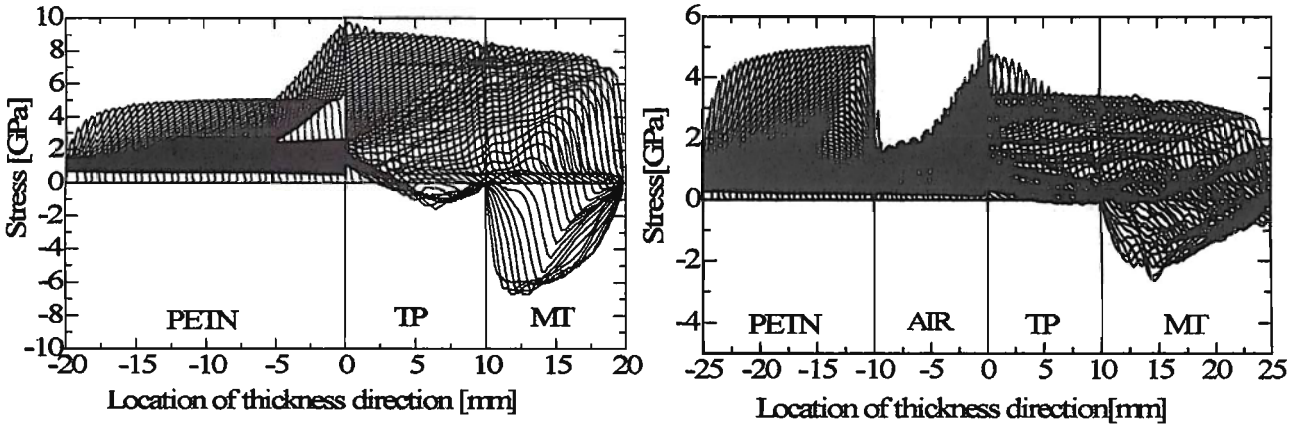

(a) 304SS (b) A2017

Figure 2. Typical numerical time histories of special stress distributions in the test assembly of (a) TP10MT10(elapsed time: 0-8.6μs) for 304SS and (b) AT(air)10TP10MT15 (elapsed time: 0-18μs) for A2017

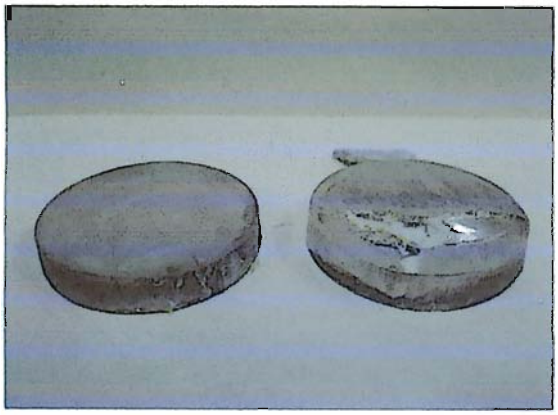

Figure 3. Typically recovered momentum trap (right) and specimen (left) plates for A2017 /TP10 MT10

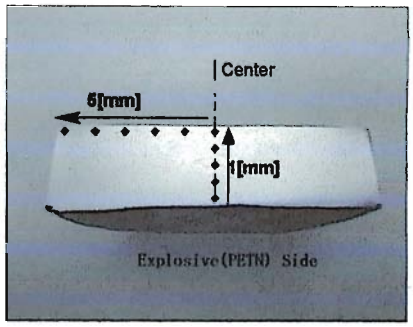

Figure 4. A typical vertical cross-section of a recovered specimen plate (A2017 /TP10MT10), showing the locations for the microhardness measurement

Damage criteria are not adopted in these calculations. It is seen that triangular compressive stress waves propagates through TP and MT, and the reflected tensile stress waves generated in MT do not transfer into TP for both cases. The gap elements are inserted numerically between TP and MT. There small tensile waves still arise in TP because of reflection of remained compressive wave tail at the emerged free surface of TP as shown in (a). The effect of attenuator, air layer is apparently shown in (b), and the incident shock pressure in TP is 53.8% of that in case of TP without AT, which almost corresponds to the numerical pressure reduction rate in cylinder explosion tests [4, 7] with an air layer between cylinder specimen and the inner explosive column. Other numerical study has reproduced experimental spall failure in MT using a damage criterion. Recovery tests of explosively compressed specimens were successfully performed inside a cushion-filled chamber without secondary damages in TP and MT. Macroscopic severe damages were not observed in almost all the TP specimens except 2-3 samples, but spall or scab damages were produced in most MT palates, as shown in Fig. 3. Such damages in MT are similar to those estimated previously by numerical simulations.

Mechanical Properties of Recovered Plates and Discussions

Microhardness. The vertical cross-section of the recovered specimens was surface-finished as shown in Fig. 4, which revealed no presence of macroscopic cracks. The microhardness of the plate was measured at an interval of 1mm axially and 5mm radially using a load of 0.98N and 15s duration at the 25 locations in total for all the specimens. Figure 5 shows a typical radial hardness distribution of A2017/TP10MT10. Generally the distributions in cases of thicker TP or MT became more uniform. All the results revealed a remarkable increase in hardness in comparison with those (144.3Hv/A2017, 237.5Hv/304SS) of virgin materials: 10.0-23.9%, 28.4-37.1%, 6.8-12.3% increases of average values per a cross-section for A2017, 304SS, A2017 (AT attached), respectively.

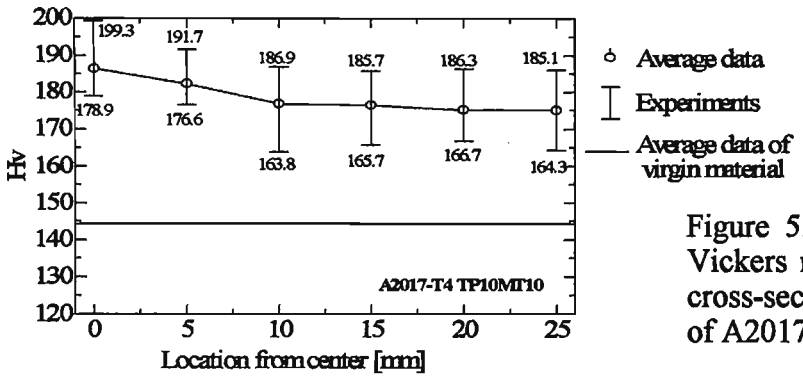

Figure 5. Typical measurement results of Vickers microhardness distributions in the cross-section of a recovered specimen plate of A2017/TP10MT10

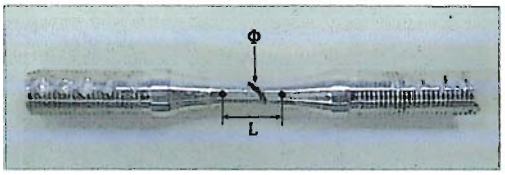

(a)

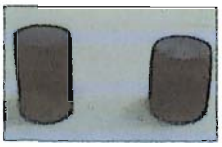

(b)

Figure 6. Typical photos of (a) a tested miniature tensile specimen (initial sizes/ ϕ :2mm, L:5mm) for A2017/TP15 MT15 and (b) small specimens (ϕ 5m, L7.5mm) before (left) and after (right) the 20% compression test for 304SS/TP15 MT15

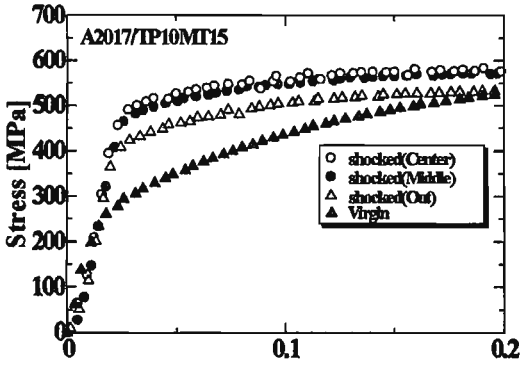

(a)

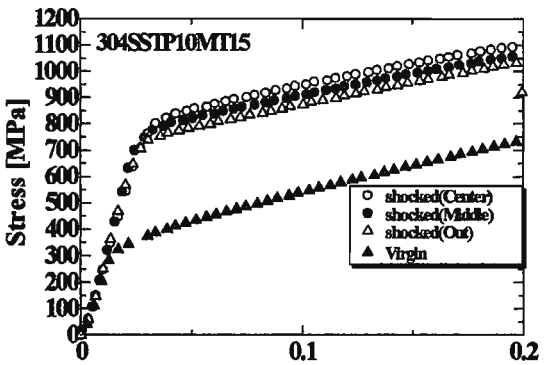

(b)

Figure 7. Typical compressional stress-strain curves obtained using small specimens machined from virgin and recovered shocked plates for the test cases of (a) A2017/TP10MT15 and (b) SUS304/TP10MT15

Tensile and compressional properties. Miniature tensile specimens (minimum tested zone / ϕ :2mm, L:5mm) and small compression specimens (ϕ :5mm, L:7.5mm) were machined parallel and vertically to plate surfaces from the recovered shocked plate specimens, and loaded to break under 2mm/min chuck velocity for tensile tests and compressed to 20% strain under the strain rate of $4.4\times10^{-3}s^{-1}$ for compression tests as shown in Fig. 6 (a), (b), using Shimadzu AG-25TB Autograph and full digital servo-hydraulic testing system FHF-EG50kN-10L. In the tensile tests, tensile strength σ_B, elongation λ and reduction of area φ (RA) were obtained measuring breaking load, elongated length between two Vickers indentations with distances of gauge length L and section area, which showed very small reduction as shown in Fig. 6(a). It is well known that the empirical proportional relation between strength [MPa] and hardness [Hv] written as equation (1) and the fracture ductility ε_f is also estimated from RA using the following equation (2), which is sometimes more effective to evaluate practical local ductile fracture than averaged elongation λ.

$$\sigma_B = C \cdot Hv \tag{1}$$

$$\varepsilon_f = \ln\left(\frac{1}{1-\varphi}\right) \tag{2}$$

Tensile tests results indicated large increase of σ_B and remarkable reduction rate of λ, φ and ε_f (ascending order) as shown in the photo of Fig. 6 (a), and $C = 2.75 - 3.16$ in Eq. 1. In the compression tests, compressive stress-strain curves were compared with those of virgin materials as shown in Fig. 7, revealing obviously different precompression effects between two materials. The results indicate that A2017 has a gradually decreasing strain-hardening characteristic, then the

differences of stress levels in the stress-strain curves between virgin and shocked materials become smaller as the strain grows, and in the contrary, 304SS which has a constant hardening characteristic

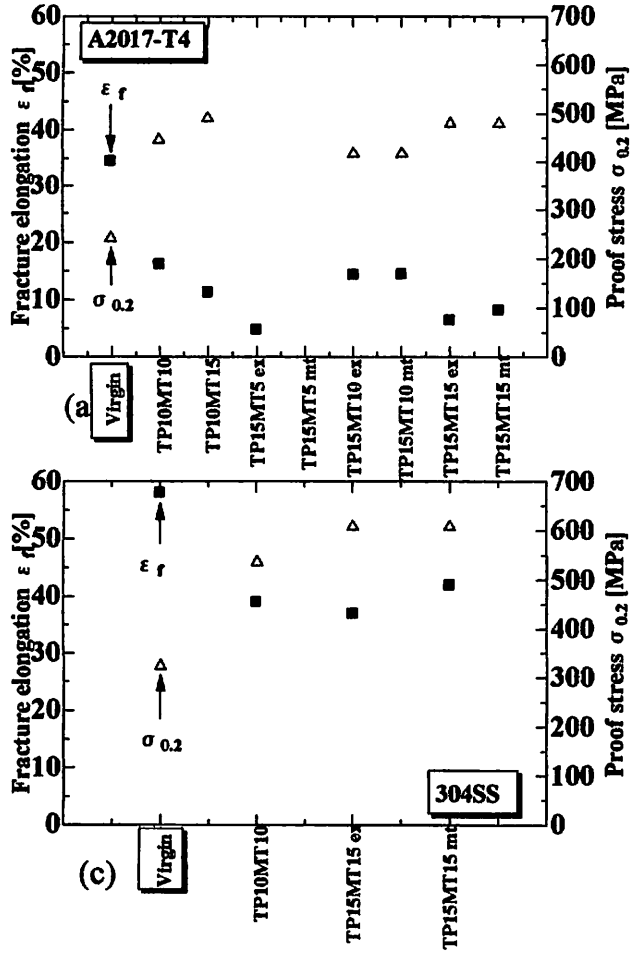

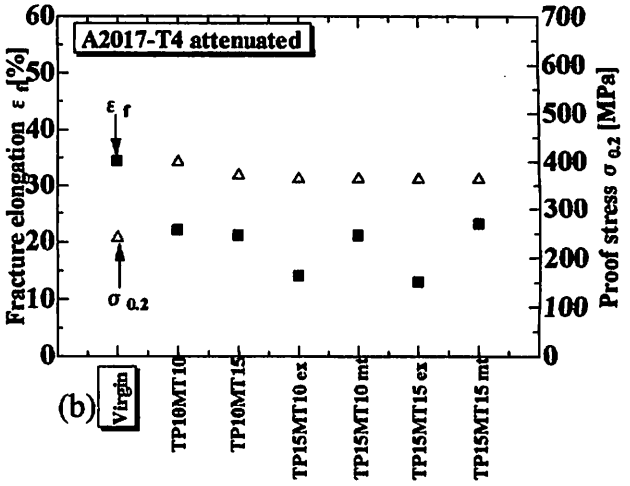

Figure 8. Mechanical properties, fracture ductility ε_f and 0.2% proof stress $\sigma_{0.2}$ obtained from tensile and compression tests, using specimens machined from virgin and recovered shocked plates of (a) A2017, (b) A2017 (shocked through attenuator) and (c) 304SS (some tests are incomplete)

shows rather upper shifted stress-strain curves. The proof stresses of 0.2% plastic strain: $\sigma_{0.2}$ are adopted as replaced yielding stresses for both materials. Figure 8 represents all the data of fracture ductility ε_f and proof stress $\sigma_{0.2}$ obtained from the tensile and compressional tests for shock-loaded specimens of A2017, A2017 (AT attached) and 304SS.

Discussions and Conclusions

In the previous study [2] on spall strength of plates shocked directly by plane detonation waves of PETN, VISAR signals indicated 262-308MPa and 352-453MPa as the spall strength σ_{SP} for A2024

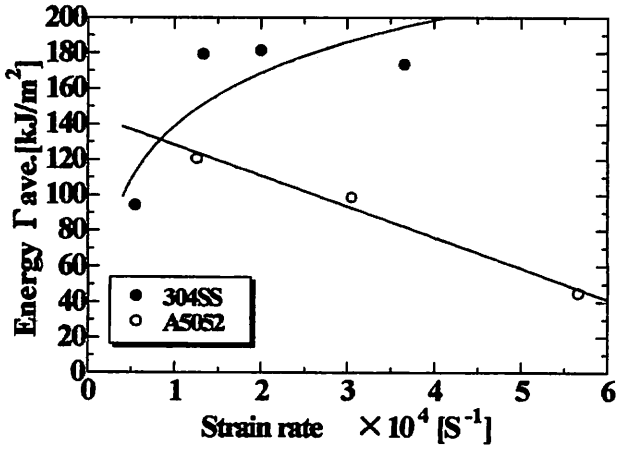

Figure 9. Relations between strain-rates and fragmentation energy [3, 4, 7] based on Grady's model and configurations of recovered fragments in explosively loaded cylinder explosion tests for A5052 and 304SS.

-T4 and 304SS respectively, which are twice to several times of static tensile strength. It has become obvious that such large increase of dynamic strength involves not only well known strain-rate effect but also basic growth of σ_B or hardness due to precompression learned in this study.

Other previous studies [3, 4, 7] on fragmentation of exploding cylinders of A5052 and 304SS driven by uniformly expanding detonation waves in inserted PETN column had revealed that the fragmentation energy Γ values estimated from the Grady's fragmentation model [6]: equation (3) using strain-rate $\dot{\varepsilon}$ of expanding cylinders and measured average width s of recovered fragments differ depending on the amount of explosives or strain-rates as shown in Fig. 9, although Γ is defined as a material constant.

$$\Gamma = \frac{\rho \dot{\varepsilon}^2 s^3}{24} \tag{3}$$

The fragmentation energy Γ of a material is often expressed [6] as a half of a product of yield stress σ_Y and critical crack opening displacement δ_C, then, the following equation (4) is obtained on the assumption that δ_C is proportional to fracture ductility ε_f.

$$\Gamma = \sigma_Y \cdot \delta_C / 2 \propto \sigma_{0.2} \cdot \varepsilon_f \tag{4}$$

Figure 9 indicates that the Γ values based on Eq. 3 descend for A5052 and increase for 304SS as the strain-rates or the amount of explosives or the intensities of precompression loads subjected to cylinder walls increase. It is noticeable that this tendency almost corresponds with the data of Fig. 8, where the ratio of the products of $\sigma_{0.2} \cdot \varepsilon_f$ in Eq. 4 of precompressed specimens to those for virgin materials are 63.9% (A2017), 84.6% (A2017/AT-attached) and 122.4% (304SS), although cylinder fragmentation phenomenon must be affected by some other factors.

References

[1] T. Hiroe, K. Fujiwara, H. Matsuo, Y. Araki and D. Nakayama: Trans. of the 15th International Conference on Structural Mechanics in Reactor Technology (SmiRT-15), Seoul, Korea, August 15-20, 1999, Vol. VII, (1999), p.161

[2] T. Hiroe, K. Fujiwara, H. Matsuo, and N. N. Thadhani: Proc. of the 4th International Symposium on Impact Engineering,16-18 July, Kumamoto, Japan, (2001), p.851

[3] T. Hiroe, K. Fujiwara, T. Abe and M. Yoshida: Proc. of 13th Biennial International Conference of the APS Topical Group on Shock Compression of Condensed Matter, July 20-25, Portland OR, USA pp. 465–472. (2003)

[4] T. Hiroe, K. Fujiwara and H. Hata: Proc. of the 16th Dynamic Behavior Related to Security Applications (DYMAT) Meeting, Brussels, 27-28 October 2005, (2005), p.159

[5] D. J. Steinberg: *Equation of State and Strength Properties of Selected Materials*, LLNL Report UCRL-MA-106439, (1991).

[6] D. E. Grady, and M. M. Hightower: *Shock-wave and high-strain-rate phenomena in materials* (Marcel Dekker, Inc.1992), p.713

[7] T. Hiroe, K. Fujiwara, H. Hata, K and H. Takahashi: To be presented at Hypervelocity Impact Society 2007 Symposium, Williamsburg, September 23-27, 2007